Phenomenological correlations in nuclear structure: an opportunity for nuclear astrophysics and a challenge to theory

R. F. Casten[1] and N. V. Zamfir[1,2]

1. Brookhaven National Laboratory, Upton, New York, 11973, USA
2. Clark University, Worcester, Massachusetts, 01610, USA

Abstract. Though it often appears daunting in its complexity, nuclear data frequently exhibits remarkable simplicities when viewed from the appropriate perspectives. This realization, which is becoming more and more apparent, is one of the fruits of the vast amount of nuclear data that has been accumulated over many years but, surprisingly, has never been completely digested. This emerging, unified, and simple macroscopic phenomenology, aided by microscopic underpinnings and physical arguments, appears in many guises and often simplifies semi-empirical estimates of structure far from stability in the critical realms where nuclear astrophysics takes place and where it is in need for improved nuclear input. The generality of simple phenomenological relationships begs both for a sound theoretical basis and for the advent of Radioactive Nuclear Beams so that the reliability of their extrapolations can be assessed and tested. These issues will be discussed, and illustrated with a number of specific examples.

1. Introduction

The data of low energy nuclear physics, which are so critical to a number of astrophysical scenarios, are both richly abundant and yet tantalyzingly lacking in key areas. Moreover, much of the data that does exist has never been conceptually digested and assimilated into the evolutionary patterns of nuclear structure. This situation is both an opportunity and a challenge. The opportunity lies in the recent, and growing, recognition that these data can be correlated in new ways that reveal remarkable simplicities, *when viewed in the proper perspective*, and that such schemes can be exploited to predict the properties of unknown nuclei. The challenge is twofold, reflecting experimental and theoretical sides of the issue. On the theoretical side, these "correlation schemes" need to be understood and justified microscopically. The simplicity they embody must point to the possibility of corresponding simplicity of understanding: the challenge is to seek out an appropriate theoretical framework. Experimentally, the advent of present and imminent generations of Radioactive Nuclear Beam (RNB) accelerators may soon open key new realms of the nuclear chart to direct empirical study.

It is the purpose of this presentation to illustrate some of the correlation schemes that emphasize and focus on the dominant role of the valence nucleons in the evolution of nuclear structure. The point, and the relevance to astrophysics, is perhaps less in the inherent interest in the particular observables to be discussed and more in the demonstration of a *type* of *approach* and in an encouragement that pursuit of this approach may yield comparable assistance for other observables.

2. Valence correlation schemes (VCSs)

It is well known that the structure of nuclei, at least at low excitation energies, is dominated by the valence nucleons. The fact that, therefore, often only a few nucleons, and their interactions, are critical simplifies many calculations, such as those in the shell model, but, at the same time, implies that nuclear phenomenology and systematics are often highly complex since the orbits occupied by the outermost nucleons change rapidly with N and Z. Classic examples of this are the phase/shape transitional regions near A = 100 and 150.

The role of the valence nucleons in phenomenology varies according to the observable, and this fact must be carefully integrated into any successful VCS that seeks to account for such phenomenology in a simple way. Albeit an oversimplification, observables may often be classified as either "mean field" or "intrinsic". The former are those characterizing the mean field ground state of a nucleus (or, occasionally, as with intruder states, of a coexisting family of states). Examples are the mass (or binding or separation energies), excitation energies or transition rates involving low-lying levels such as the 2_1^+, 4_1^+ states that act as signatures of the mean field structure. The latter characterize intrinsic excitations (e.g., non-rotational states in deformed nuclei) such as β, γ, or octupole excitations.

Mean field observables generally depend primarily on the properties of the valence nucleons, taken as an ensemble, although the occupation of specific orbits can sometimes play a dramatic role. Particularly important for these nuclear properties is the valence residual p-n interaction. An illustration of this is provided in Fig. 1 which shows $E(2_1^+)$ values for nuclei in the Sn region. For Sn, which is proton magic, the structure is virtually independent of the number of (valence or total) neutrons. This is a characteristic property of a system with good seniority. However, as soon as valence protons are added to (or subtracted from, as holes) the system, yielding elements such as Te, Cd, or Xe, $E(2_1^+)$ drops rapidly in energy as the number of valence neutrons is increased (up from N = 50 or down from N = 82). The reason is, in major part, due to the importance of valence p-n interactions. It is to be noted, for example, that $E(2_1^+)$ for Xe, which has N_p = 4 (4 valence protons) is lower than for Te (N_p = 2) for the same neutron number since Xe has twice as many individual p-n interactions and therefore much greater tendency to break seniority and to build up collectivity.

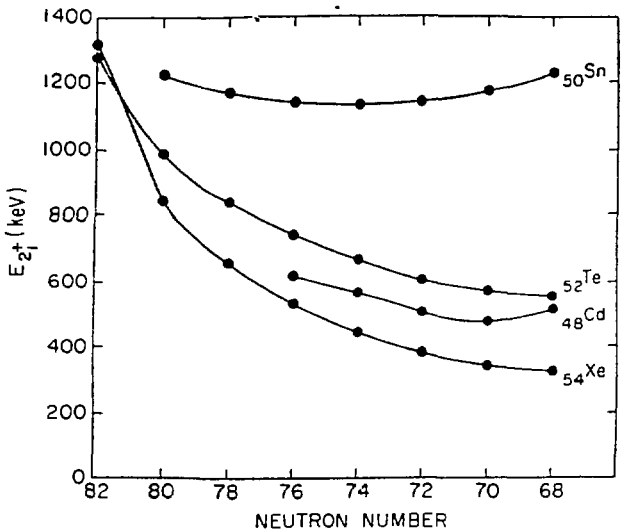

Fig. 1 2_1^+ energies in the Sn region.

In contrast to mean field attributes, intrinsic excitations are generally constructed by operating on the mean field wave functions with some characteristic operator (e.g., $r^2Y_{2,\pm2}$ for the γ vibration), and the resulting properties of these excitations depends on which single particle (or quasi-particle) orbits give large excitation matrix elements. The phenomenology of such excitations thus depends on which nuclei witness the filling of these orbits and their presence near the Fermi surface.

We will illustrate below the processes of constructing VCSs for both types of observables, but will focus mostly on those of mean field type as they are frequently of more immediate astrophysical interest.

2.1 The N_pN_n scheme and the P-factor

As we indicated earlier, nuclear data is often bewildering in its complexity. This is illustrated on the left in Fig. 2 which shows 2_1^+ energies in the A = 100 region. Large values of $E(2_1^+)$ are typical near-closed shell nuclei exhibiting only weak collectivity. Smaller values signify the transition to more collective vibrational and, ultimately, deformed nuclei. The phenomenology of Fig. 2 clearly shows a large range of $E(2_1^+)$ values and hence a variety of structures but certainly does not disclose any simple way to "see" this structural evolution. Of course, detailed models can be applied to regions like this and have successfully described the spherical-deformed transition region near A = 100 so that the details of Fig. 2 can be understood: for example, the transition occurs most rapidly in Sr, Zr, less so in Mo and hardly at all in Pd. Yet such detailed calculations, though they are valuable, belie the point of seeking a simple ansatz for the systematics and are seldom done in the

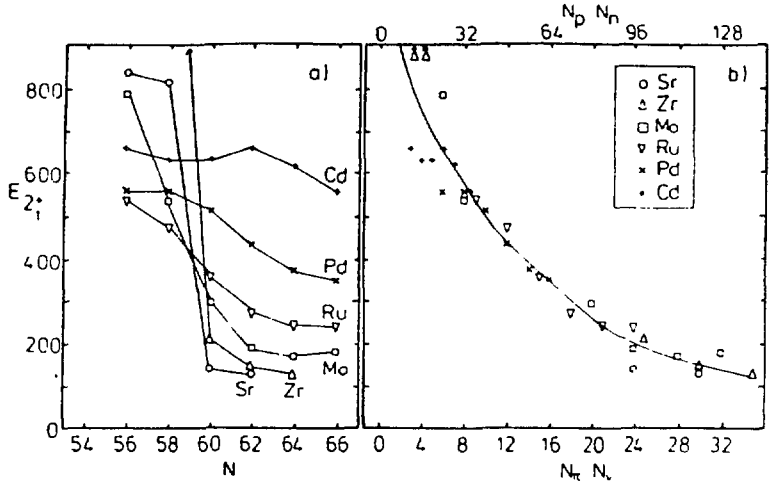

Fig. 2 Normal and N_pN_n plots for the A ~ 100 region.

absence of sufficient pre-existing data for a given region that its structural features are already clear.

We take a different approach. If the valence p-n interaction is indeed critical to the development of collectivity, there should be some relatively simple quantity that embodies this fact. If we assume that the p-n interaction is orbit-independent (a rough approximation but one which is approximately confirmed empirically) than the total, integrated, strength of the valence p-n interaction is simply given by the product of the number of valence protons, N_p, and the number of valence neutrons, N_n; that is, by the valence product N_pN_n. Note that N_p and N_n are counted, either as particles or holes, to the nearest closed shell. Plots of mean field observables against N_pN_n are the essence of what is known as the N_pN_n scheme [1]. The right side of Fig. 2 illustrates the N_pN_n scheme for $E(2_1^+)$ value near A = 100. Evidently, there is a profound simplification. Similar plots are obtained for other observables such as $E(4_1^+)/E(2_1^+)$, $B(E2{:}0_1^+ \rightarrow 2_1^+)$ and the like. The only caveat in constructing such plots is that attention must be paid to the presence, and evolution, of important subshell closures which affect the counting of valence nucleons. The A = 100 region provides a nice example of this that has been well known for fifteen years. For nuclei with N<60 there is a significant proton gap at Z = 38. However, this gap disappears suddenly (another effect of the p-n interaction) for N≥60, leaving behind the traditional Z = 28-50 shell. [A similar effect occurs for Z = 64 in the A = 150 region, which disappears [2] for N≥90.] The N_pN_n scheme can be applied to many regions of nuclei and, in general, has been successfully exploited for A≥80. The microscopic ansatz underlying it, the average constancy of the p-n interaction, has been empirically verified, at least for the upper and lower thirds of major shells. The observed decrease in average p-n interaction

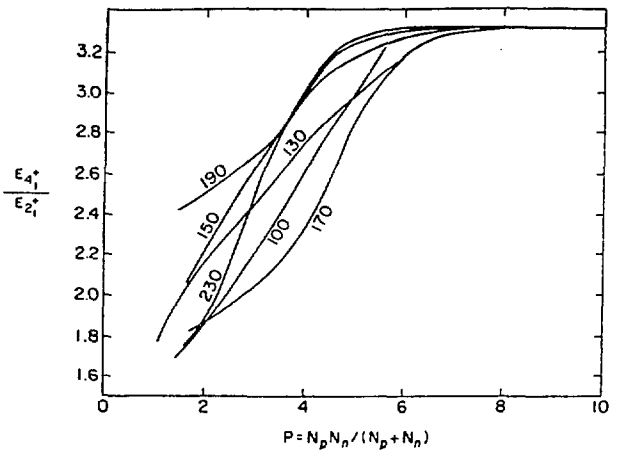

Fig. 3 P-plots of the $4_1^+/2_1^+$ energy rates for six regions of medium and heavy nuclei. The curves are smooth lines drawn through the data points in NpNn plots for each region (see ref. 3).

strengths in the middle third shell region, accounts for a number of "saturation" phenomena in which quantities such as $E(2_1^+)$ and $B(E2:0_1^+ \rightarrow 2_1^+)$ values become asymptotic near midshell. Many N_pN_n plots have been shown in the literature and need not be repeated here. Rather, we will turn to some newer results of more current topical interest.

One aspect of the N_pN_n scheme is that there is no obvious interpretation of a particular numerical value. For example, does a value $N_pN_n = 120$ imply a collective deformed nucleus or not? This may depend on a particular region. It would be nice to have a related quantity whose absolute value conveys some more precise physical idea.

This goal is the motivation behind the P-factor which is defined [3] as

$$P = \frac{N_pN_n}{N_p+N_n} \qquad (1)$$

P can be thought of as a "normalized" N_pN_n. It is the number of p-n interactions *per* valence proton or neutron. More significantly, perhaps, it is the number of valence p-n interactions divided by the number of pairing interactions and is therefore proportional to the ratio of *integrated* p-n to pairing interaction strengths. For example, a P value of 5, which, for reasons that will become obvious, we call P_{crit}, corresponds to 5 p-n interactions for every pairing interaction. Since typical p-n matrix elements are ~0.2 MeV, and the pairing interaction strength is ~ 1 MeV, $P_{crit} \sim 5$ corresponds to just the point at which the p-n interaction strength begins to dominate the pairing strength. It is, then, hardly surprising that virtually all regions of heavy nuclei become deformed for nuclei with P values near

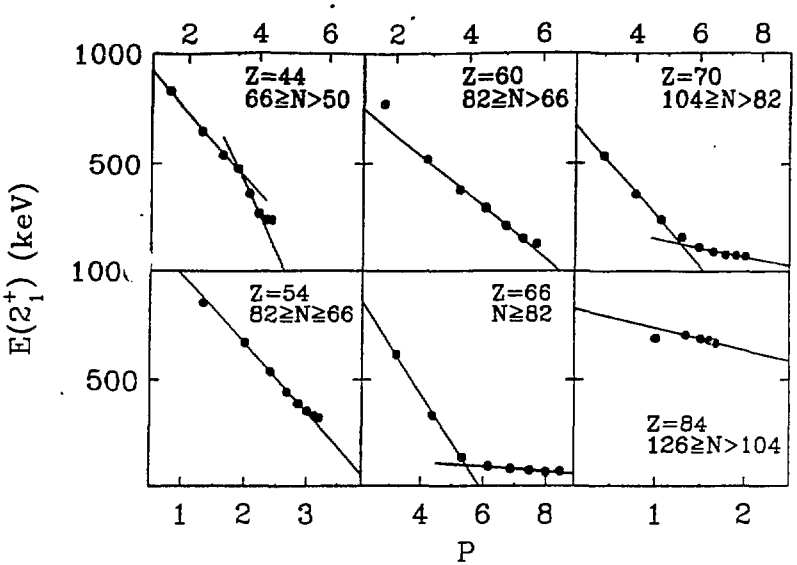

Fig. 4 Plots of $E(2_1^+)$ values against P for typical elements (based on ref. 4).

P_{crit}. This is shown in Fig. 3 which combines, in one view, the individual P-plots (indicated by smooth lines drawn through the envelope of points in each plot) of $E(4_1^+)/E(2_1^+)$ for 6 regions. It is clear that, first, all the regions have basically the same shape and, secondly, that absolute values of P, especially near P_{crit}, have an important physical meaning and significance.

Generally, the behavior of a given observable against N_pN_n and P, in a given region, is rather similar although, for reasons not yet fully understood, sometimes the patterns are quite different, and this can often be a useful feature. Energies of 2_1^+ levels, for example, which coalesce in a compact envelope against N_pN_n are not nearly so well-behaved against P. However, the P-plot in its own way discloses a fascinating correlation for $E(2_1^+)$, namely, that, for a given *element*, a plot of $E(2_1^+)$ vs. P is very accurately linear [4] in a given major shell. Plots of $E(2_1^+)$ against P often split into two *separate* linear segments, with different slopes, for $P<P_{crit}$ and $P>P_{crit}$. This phenomenology, which has been shown to extend from Zr to the actinides, is illustrated for a few cases in Fig. 4.

A particularly important ingredient in astrophysical calculations (e.g., of the r-process) is nuclear masses (or binding or separation energies). The P-factor has been shown [5] to be useful here as it linearizes the microscopic, non-liquid drop, component of the mass rather well. This is illustrated in Fig. 5 which shows P-plots for several sequences of semi-empirical microscopic (SEM) masses for the actinide nuclei, that is, measured masses corrected for their liquid drop component. The P-factor gives, in a single parameter scheme (the slope), a correlation of the masses at least as good as many of the best mass equations. Moreover, as shown in

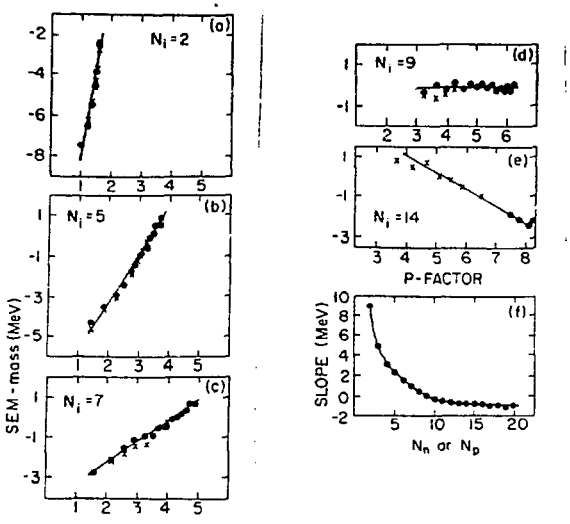

Fig. 5 Semi-empirical microscopic (SEM) masses plotted against P for isotopic (dots) and isotonic (crosses) sequences in the actinide nuclei. N_i gives the (constant) value of either N_p or N_n in each plot. Panel (f) plots the observed fitted shapes against N_p or N_n (from ref. 5).

the lowest panel, the slopes behave very smoothly, decreasing monotonically as either N_p or N_n (for isotopic and isotonic sequences, respectively) increases. This comment, of course, is not meant to denigrate the latter, for they are frequently microscopic and much more global in scope, but, at the same time, they typically involve a large number of parameters. As a purely *practical* guide to masses, the P-factor would seem to compete well, in particular regions, with more complex schemes.

2.2 Identical bands and the P-factor

The above discussion of the linearity of 2_1^+ energies with the P-factor in isotopic chains has a direct bearing on the recently active topic of "identical bands" (IB) which are rotational bands in pairs of nuclei (either even-even pairs or an even nuclei and its adjacent odd-even nucleus) with virtually identical energy spacings [6,7]. It has been shown [8-12] that such IBs, first discussed in high-spin superdeformed states, are widespread at low spin as well. For our purposes we restrict the following remarks to pairs of even-even nuclei at low spin. For these, it has now been noted that the IB phenomenon need not concern only adjacent nuclei but that widely dispersed nuclei can have identical bands as long as they have similar N_pN_n values [11]. This should not be surprising since, if $E(2_1^+)$ is smooth against N_pN_n or P, then rotational spacings, E(J)-E(J-2) might well be also. Thus, the linearity of $E(2_1^+)$ with P (and similar results for other yrast spins) implies not

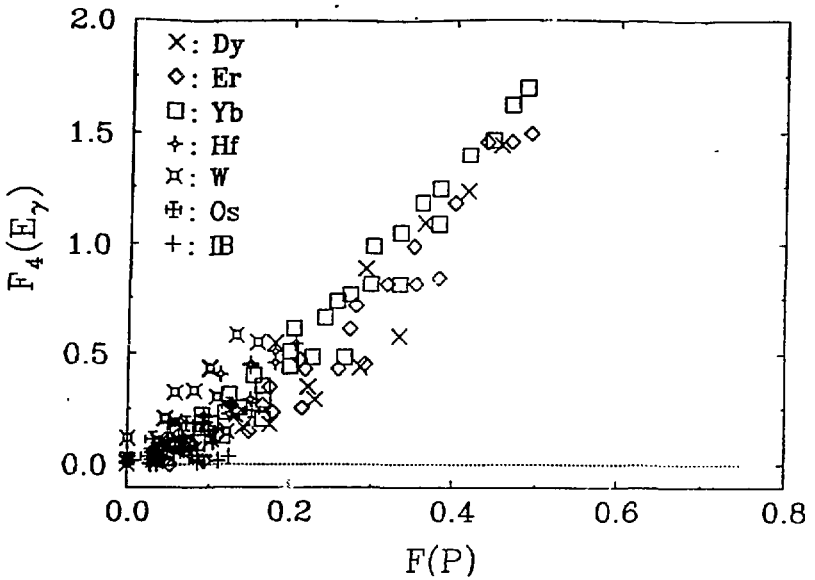

Fig. 6 Fractional change in the 4_1^+–2_1^+ energy spacing for pairs of nuclei plotted against the fractional change in P. The nuclei included are the pairs of identical band nuclei in ref. 11 and pairs within the isotopic sequences of nuclei from Dy-Os (from ref. 12).

only that nuclei with similar N_pN_n or P can have similar rotational spacings but also that the IB phenomenon is *not* a special characteristic of a few singular nuclei that are somehow qualitatively different than others. Rather, rotational energies should vary smoothly with P in an isotopic chain. The IB phenomenon is the terminus of a continuous variety of rotational behavior. This idea is demonstrated [12] in Fig. 6 in which the *fractional change* in $E(4_1^+)$-$E(2_1^+)$ is plotted, for some IB pairs of nuclei and for nuclei in a number of isotopic chains, against the fractional change $[(P_2-P_1)/(P_2)]$ in P between nuclei 1 and 2. Not only is the envelope of points smooth and rather compact, but it is nearly linear. This result suggests that a key ingredient in understanding IBs at low spin is the competition between pairing and the p-n interaction.

2.3 Interpolation vs. extrapolation and astrophysics

It is often critical in astrophysical applications of nuclear physics to know and use the values for some (or several) observables in nuclei far from stability where the relevant data are not known. Traditionally, this entails a risky process of extrapolation or the generally equally risky use of a model prediction. The dangers inherent in this are evident if one tries to extrapolate 2_1^+ energies on the left in Fig. 2. Or, to take a more dramatic

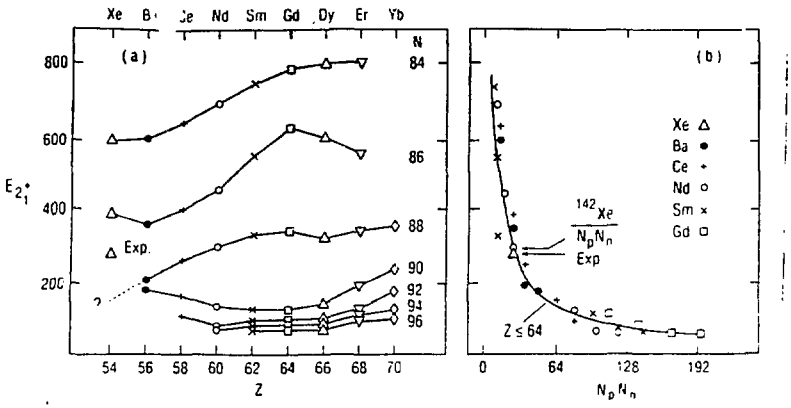

Fig. 7 Normal and N_pN_n plots for the A~150 region along with the recently measured data point for ^{142}Xe (from ref. 13).

example, to have tried to do so for ^{100,102}Zr or ^{98,100}Sr (N = 60,62) *before* these isotopes were studied in the 1970's. The N_pN_n and P-factor schemes simplify this process in two ways. First, the systematics is smoother and "tighter" so extrapolation (see Fig. 2, right) is more reliable. Secondly, and often far more importantly, these schemes often *turn the process of extrapolation into one of interpolation.* The reason is simple to see by an example. Consider Fig. 7 and the case of $^{142}_{88}$Xe, until recently [13] a nucleus with unknown $E(2_1^+)$. To guess $E(2_1^+)$ for ^{142}Xe in the normal plot on the left is not easy. The contour for N = 88 is sloping down for lower Z values, pointing toward a 2_1^+ energy of, perhaps, about 150 keV. On the other hand, the approach towards Z = 50 suggests that, perhaps, the 2_1^+ energies might begin to rise as Z decreases. This seems the case for N = 86 at least and could suggest a value near 300 keV for ^{142}Xe. Clearly, quite a range of uncertainty is presented.

However, note what happens in the N_pN_n scheme. In this region, nuclei are known with N_pN_n as large as 192. A well known nucleus such as ^{154}Sm, for example, has N_p = 12, N_n = 10, and hence N_pN_n = 120. In contrast, the *unknown* nucleus ^{142}Xe has N_p = 4, N_n = 6, and, hence, N_pN_n = 24. To predict its properties in the N_pN_n scheme is an *inter*polative process entailing merely reading the value off an *already existing* curve. As is evident in Fig. 7, right, this process works exceedingly well. It has been tested in other nuclei as well, and also for $E(4_1^+)/E(2_1^+)$ratios.

Such a technique may be particularly useful in providing input to the Saha partition equations in r-process network calculations. The discussion in section 2.1 suggests that similar interpolative advantages may arise in the N_pN_n or P-factor approaches for nuclear masses as well[5].

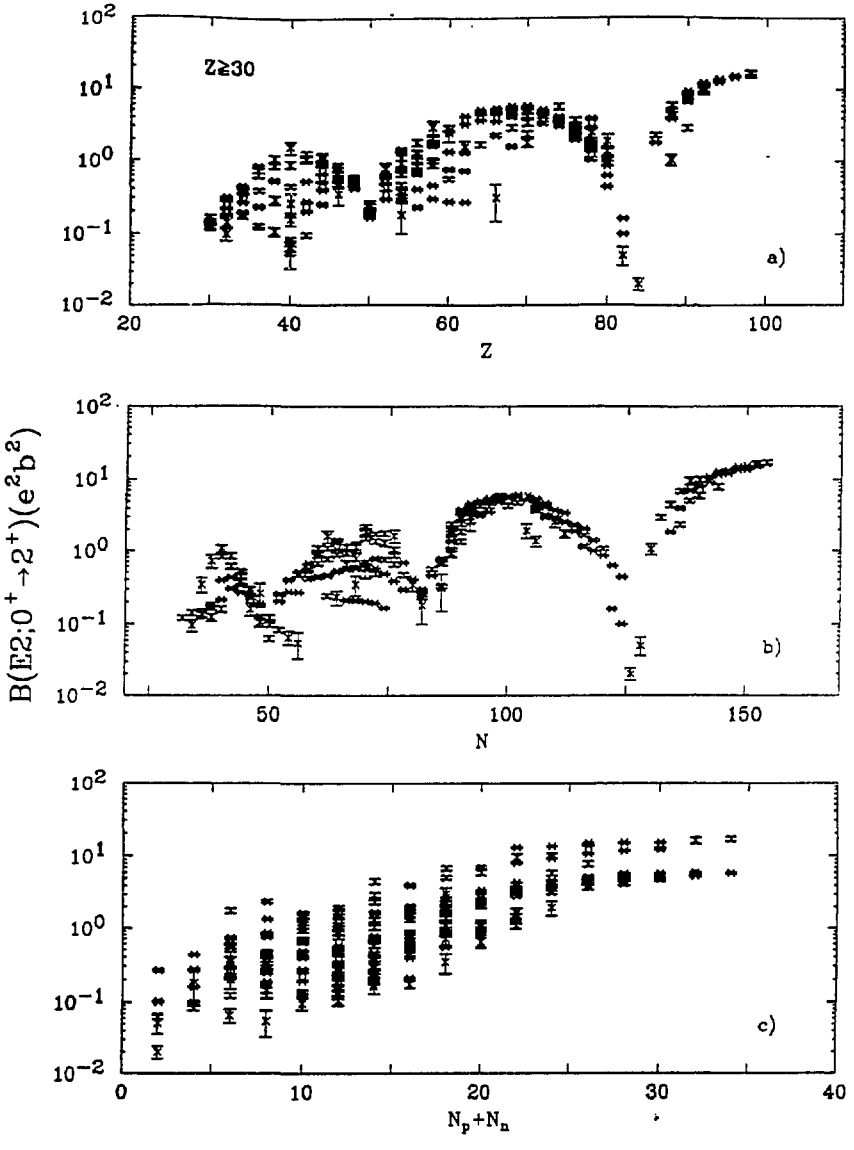

Fig. 8 $B(E2:0_1^+\rightarrow 2_1^+)$ values in e^2b^2 plotted against three variables.

2.4 A case study: the saga of $B(E2:0_1^+\rightarrow 2_1^+)$

To return to the general process of exploiting VCSs to simplify and assimilate the vast amount of nuclear data currently available, we now turn to discuss a particular observable, $B(E2:0_1^+\rightarrow 2_1^+)$ values, which are a critical measure of collectivity, in more detail in order to illustrate a kind of iterative or sequential process whereby their phenomenology is successively rendered

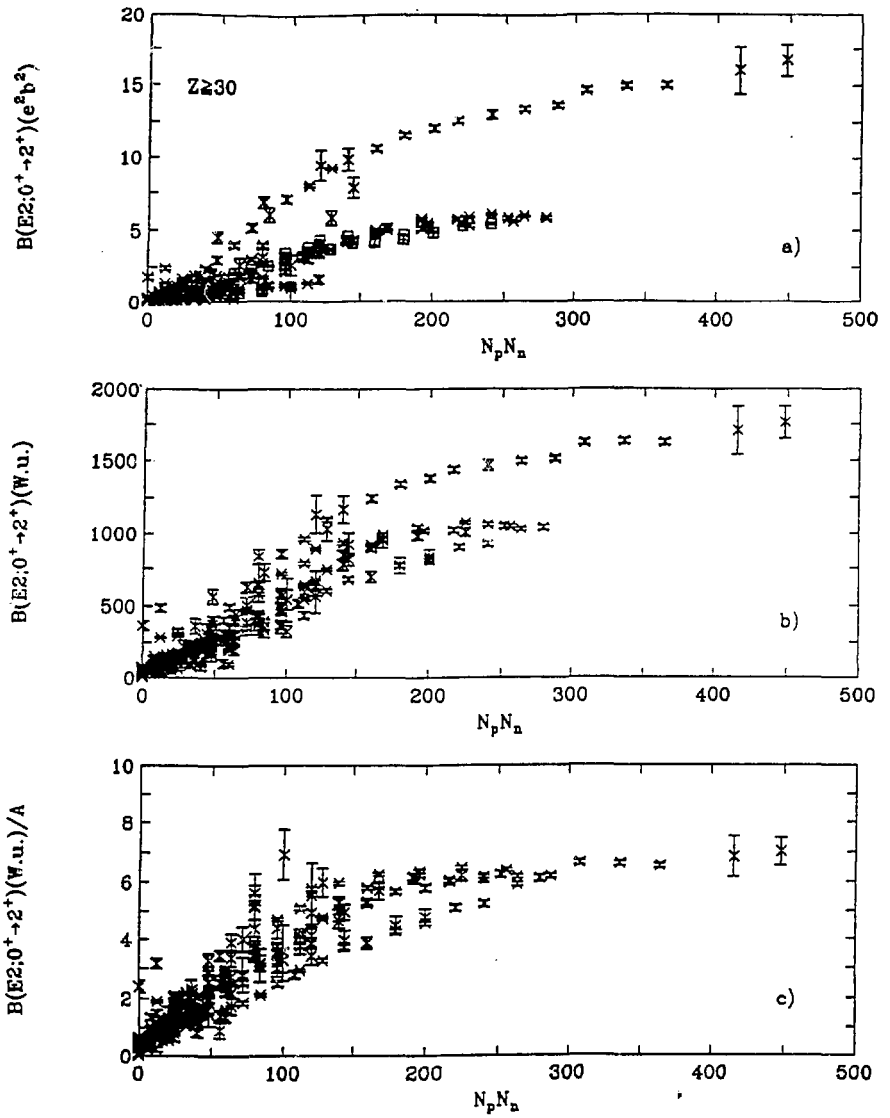

Fig. 9 a) $B(E2:0_1^+ \rightarrow 2_1^+)$ values in e^2b^2 plotted against N_pN_n.
b) Same as Fig. 9a except the B(E2) values are in W.u.
c) Same as Fig. 9b except the B(E2) values are divided by A.

simpler and simpler. For this purpose we rely on the superb recent compilation of these values by Raman et al. [14].

Figures 8a,b show $B(E2:0_1^+ \rightarrow 2_1^+)$ values for all even-even nuclei with $Z \geq 30$, plotted against neutron and proton number. While there are certainly some visible trends, especially in the rare earth and actinide regions, the

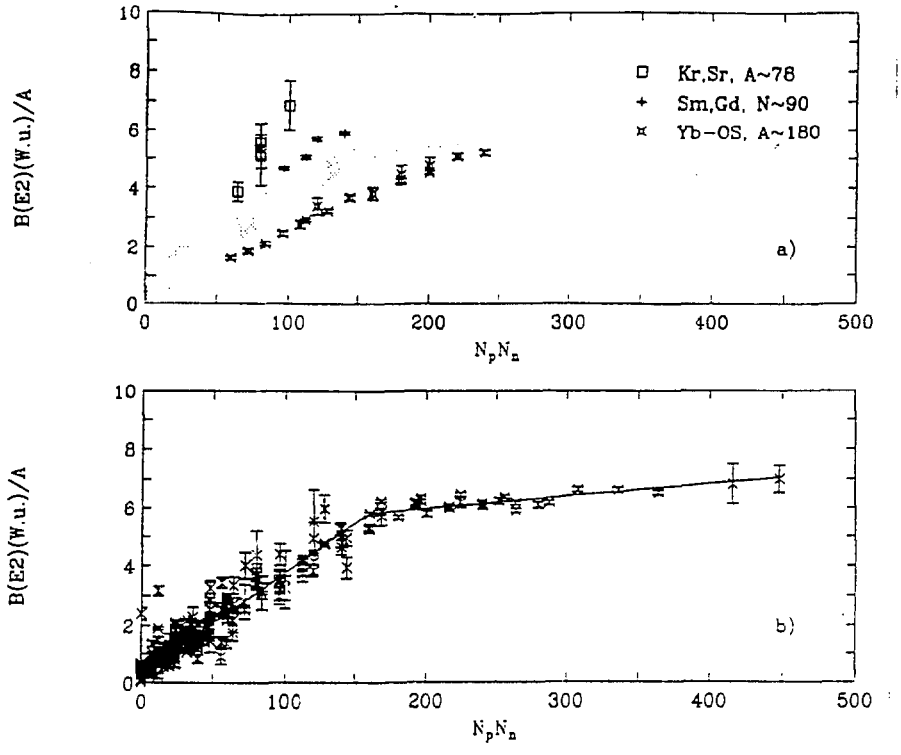

Fig. 10 a) Schematic drawing of the trends in Fig. 9c, highlighting the global behaviors and the "deviant" nuclei. b) Same as Fig. 10a, but without the deviant nuclei. The straight lines are two linear fits to the data.

overall patterns are murky and, in substantial portions of the plot, are utterly chaotic. Figure 8c shows a plot against the sum of N_p and N_n, that is, the total valence nucleon number. If anything, the trends are less clear. Figure 9a, however, shows that a major simplification occurs if these B(E2) values are plotted against N_pN_n. This may not be surprising given the foregoing, but it must be remembered that, now, we are comparing many different *regions* on the same plot. Smoothness of B(E2) values against N_pN_n in one region does not in itself ensure any particular relation between regions. Yet Fig. 9a is a distinct improvement over Fig. 8. Still, however, there are several distinct "strings" of values. A further substantial improvement occurs if, as in Fig. 9b, the B(E2) values are expressed in Weisskopf units (W.u.) instead of absolute units (e^2b^2). The A dependence embodied in the W.u.is $A^{4/3}$: this arises from the r^2 dependence of the E2 operator and the fact that $B(E2{:}0_1^+ \rightarrow 2_1^+) \propto Q^2$. Incorporating this expected dependence further simplifies the plot. However, there is still a clear residual structure to the plot. Further inspection reveals that there is an A dependence. In Fig. 9c we

therefore arbitrarily divide the B(E2) values in W.u. by A. Now, nearly all the data for ~200 nuclei collapse into a narrow envelope.

There are still, though, a few recalcitrant nuclei. To proceed further, we now need to identify these more specifically. Figure 10a does so by schematically indicating the overall trend of Fig. 9c and labelling the nuclei deviating from it. It is seen that they are not randomly distributed but fall into 3 groups, the W-Os nuclei in the A ~ 180 region, the N = 90,92 isotopes of Nd-Gd, and a few isotopes of Sr and Kr with N = 38-42. Note that the first group exhibits lower B(E2) values, while the latter two show values higher than the general trend. Once these special nuclei are identified, it is possible to understand why they are different. These are nuclei for which large hexadecapole deformations have either been measured [15,16] or suggested from potential energy surface calculations [17]. Intriguingly, the Nd-Gd region has $\beta_4 > 0$ while the W-Os nuclei have large negative β_4 values. We can see the effect these shape components have if we recall the expression for the quadrupole moment in the presence of quadrupole and hexadecapole deformations, namely,

$$Q \propto \beta_2 \, [\, 1 + 0.360\, \beta_2 + 0.967\, \beta_4 + 0.328\, \beta_4^2/\beta_2 \,] \qquad (2)$$

Hence, the first order effect of a negative β_4 is to reduce Q while a postive β_4 increases Q. Since $B(E2) \propto Q^2$, significant β_4 values may modulate the B(E2) values. The magnitude of the effect (using known β_4 values) is not quite sufficient to explain the full deviations of the B(E2) values of these nuclei from the general envelope in Fig. 9c, but it is in the correct direction and accounts for a significant fraction of the effect. Further effects due to higher order or other shape components (e.g., β_6, γ) may be relevant as well. Indeed, these nuclei are known to be γ-soft and some display coexisting states of different shapes (e.g., prolate and oblate). The main point here is that the generation of a simple systematics, obtained by plotting B(E2)(W.u.)/A against N_pN_n, helps highlight, identify and isolate exotic nuclei as well as to simplify the phenomenology for others.

If these few "badly behaving" nuclei are removed from Fig. 9c, the final plot shown in Fig. 10b, incorporating ~185 nuclei, is obtained. The route from Fig. 8 to Fig. 10b is a case study in the benefits that can accrue from a simple analysis in terms of VCSs. We are left with two interesting physical results. First, the data in Fig. 10b can be superbly fit by an extremely simple exponential or linear expression. This is clear from inspection of the two straight line segments in Fig. 10b. Reproduction of this analytic expression (either form, since the linear expression can be thought of as the first term in an expansion of the exponential) is a critical challenge to microscopic theories of nuclear structure. [We note that Raman et al. [18] and Frank et al. [19] have developed similar empirical formulas in N_pN_n for individual regions but did not remark on their more global aspects as these were not so evident in plots of B(E2) values in units of e^2b^2.] The second result referred to above is this extra A dependence beyond that expected from the single

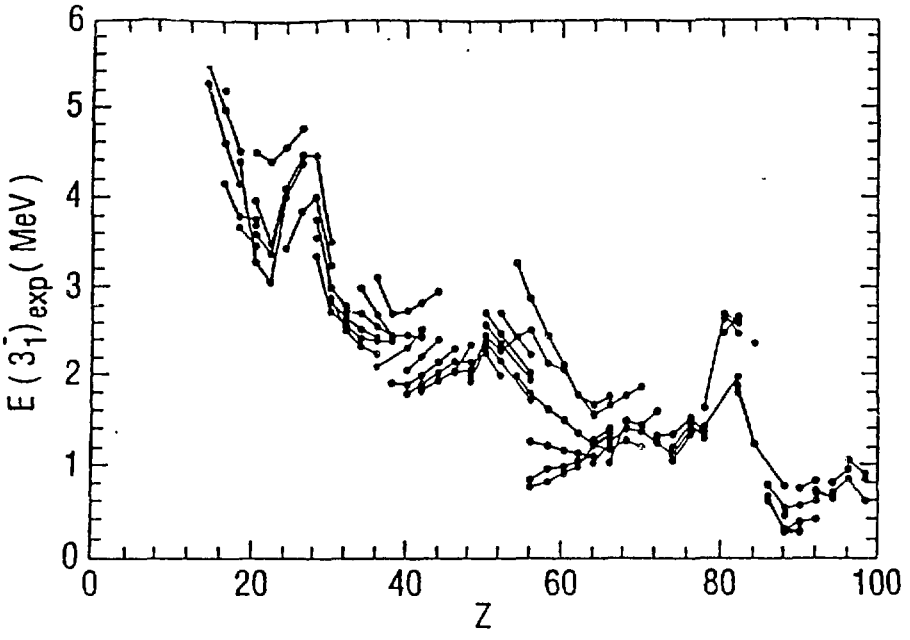

Fig. 11 3_1^+ energies plotted against Z (from ref. 21).

particle unit itself. This is surely a critical factor to be explained microscopically. We note in passing that a plot of $B(E2:0_1^+ \rightarrow 2_1^+)$ (W.u.)/Z against N_pN_n is equally simple. Finally, we note that the relevance of such a simple expression would never have been so clear in a normal plot such as Fig. 8. It was only through the mediation of an appropriate VCS that the ultimate simplicity emerged.

2.5 Intrinsic excitations

We shall be much briefer here, not because VCSs are less useful in this context but because such excitations (with the exception of the GDR) are seldom very important in astrophysics. Nevertheless, the ideas are relevant for any processes involving single particle-type matrix elements such as β decay which *is* critical, for example, to the r-process. The idea, as before, is, of course, to base a correlation scheme on the inherent properties of the observable. For β decay, this will be difficult and has not yet been successful, but the illustration of the idea may, hopefully, be "inspirational". For this purpose, we discuss octupole excitations and, in particular, the lowest 3^- state. Although the nature of this state varies enormously between, for example, vibrational and deformed nuclei or within deformed nuclei, depending on whether K = 0, 1, 2, or 3 excitations are lowest, we will still attempt a unified treatment [20]. Normal plots of 3_1^- display complex structure as seen in Fig. 11.

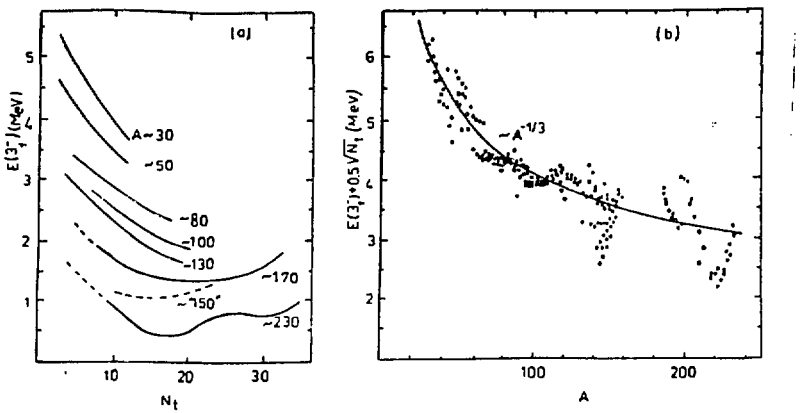

Fig. 12 a) Smooth curves drawn through trends of 3_1^- energies for the mass regions indicated, plotted against N_t. b) The 3_1^- energies correct for an N_t dependence plotted against A (from ref. 20).

Octupole intrinsic excitations are "created" (in the RPA or TDA sense) by an operator of the form r^2Y_{3K}. The energy and collectivity of the 3_1^- state will depend on where (in N and Z) there are the largest (and greatest number of) matrix elements of Y_{3K} connecting single-particle or quasi-particle states near the Fermi surface. Favored matrix elements of this operator connect states with $\Delta l = 3$ and, of course, opposite parity. The largest matrix elements therefore will be those in which single-particle states, differing by $\Delta n = 1$, $\Delta l = 3$, and $\Delta j = 3$, are clustered near the Fermi surface. This occurs once in each major shell due to the single-particle spin orbit interaction which brings one orbit (the so-called "unique" or "non-normal" parity orbit) down in energy so that, increasingly with A, it penetrates into the midst of the opposite parity orbits of the next lower major shell. For neutrons (protons) in the rare earth region, this orbit is the $\nu i_{13/2}$ ($\pi h_{11/2}$). It occurs in these nuclei rather near the $\nu f_{7/2}$ ($\pi d_{5/2}$) orbit, forming the appropriate $\Delta l = \Delta j = 3$ pair. In the deformed field, of course, each of these single particle states breaks up according to the K projection value. Early in the deformed region, the favored octupole states have K = 0,1 and thus Nilsson orbits of opposite parity with $\Delta n_z = 3$, $\Delta K = 0,1$ are the favored construction material for these emerging collective states. Later on, higher K values dominate. For brevity here, we discuss only the low K region. References 20 and 21 provide a fuller treatment.

It is evident, then, that the lowest octupole states will decrease in energy as a shell fills until one (usually the normal parity) of the critical $\Delta l = 3$ orbit pairs is filled, thus maximizing the ability to create $\Delta l = 3$ quasi-particle excitations to the other orbit. Beyond this point, the octupole energy increases as occupation of the upper $\Delta l = 3$ orbit (usually the unique parity) begins to fill, blocking the needed quasi-particle excitations. Hence it is clear

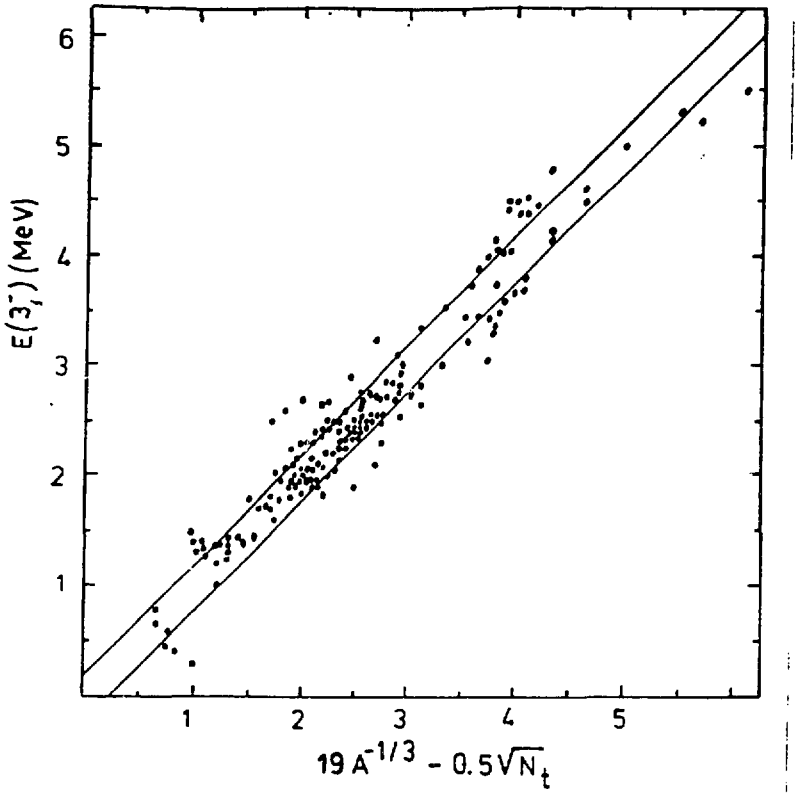

Fig. 13 Empirical 3_1^- energies plotted against eq. 3. The diagonal lines give the bounds corresponding to ± 200 keV deviation from this formula.

that the controlling parameter is simply the degree of shell filling. This process occurs in parallel for protons and neutrons and so it is intriguing to plot $E(3_1^-)$ simply against $N_t = N_p + N_n$. We do this in Fig. 12a for nuclei from A ~ 30 to the actinides. Nearly all the curves for individual regions are parallel, at least up to N_t ~ 26 where the rare-earth and actinide data rise again due to filling of the unique parity orbit. The only exceptions to this consistent behavior are the shape transitional A ~ 150 and Ra-Rn regions (dashed). These special regions can be understood, but a full discussion [21] is beyond the scope of this presentation and not particularly relevant to the generic point being made. Henceforth, then, we will omit these two small groups of nuclei. Clearly the remaining nuclei show two characteristic features, namely a smooth N_t dependence and an A dependence. A little analysis shows that the N_t dependence can be described by the function -0.5 $\sqrt{N_t}$ (MeV). Figure 12b "corrects" the 3_1^- energies by this term in order to isolate the A dependence which is seen to be of the form $A^{-1/3}$. Thus, we can now parameterize 3_1^- energies by the simple expression

$$E(3_1^-) = 19A^{-1/3} - 0.5\sqrt{N_t} \quad (3)$$

Figure 13 plots this formula against the data (perfect agreement corresponds to points along the diagonal line) for all non-closed shell nuclei with A > 30 and N_t < 26 except for the aforementioned A = 150 and Ra-Rn nuclei. It is clear that eq. 3 provides a very fine, and remarkably simple, representation of the data. Over 2/3 of the 165 data points, spanning 3_1^- energies from less than 1 MeV to more than 5 MeV, are reproduced to better than 200 keV. These results can be improved upon by a slightly more sophisticated analysis, but the point remains that a simple VCS works well for this example of an intrinsic excitation as well.

3. Radioactive Nuclear Beams (RNBs)

Intriguing as these phenomenological schemes are, they are merely theoretical constructs and, being phenomenological, are always subject to microscopic "surprises", such as changes in shell gaps (e.g., Z = 64-type effects). That is one key reason why a microscopic understanding is so urgently needed. But equally or more important, it is critical to actually measure many of these structural properties far from stability to test and refine the above ideas and to garner more data for other observables. This is an aim of the active on-going initiative for RNB facilities worldwide. The experimental programs at these facilities will open up wholly new horizons and provide a more solid empirical basis for the nuclear input to astrophysics. There is no need to discuss these initiatives in detail here as this has been, and is being done, elsewhere (see ref. 22). Suffice it to note two important recent developments in North America, the RIB facility at Oak Ridge currently under construction, and the Isospin Laboratory (ISL) which is being actively pursued. These will provide much of the data nuclear astrophysics requires and should greatly expand both nuclear structure and astrophysical horizons.

4. Conclusions

There are four principal conclusions to this discussion. One is the tremendous need, experimentally, for more data on nuclei far from stability if nuclear astrophysics is to reduce the uncertainties involving its nuclear input so that it can focus on astrophysical issues. This will require extensive effort to develop and use accelerator complexes, such as the first-generation facility RIB at Oak Ridge or the second-generation broad-range facility ISL.

Secondly, Valence Correlation Schemes (VCSs) can provide extremely powerful phenomenological tools to assimilate, correlate, and, at some non-trivial level, to understand the rich and complex phenomenology of a significant number of key nuclear structure observables. At the same time they provide a new tool for nuclear astrophysics, with which values of

nuclear observables may be extracted and the correlations in these vividly highlighted.

Thirdly, these studies point to the inordinate usefulness and importance of "horizontal" compilations and evaluations of specific observables over broad ranges of nuclei. It is often only with such work (often laborious and tedious) in hand that many of the beautiful systematics of nuclear structure really emerge. Indeed, it is hard to think of an example of such a compilation effort that did not ultimately reap enormous benefits both to nuclear structure and to allied fields such as nuclear astrophysics. The examples provided by Sakai [23] and, more recently, by Sood, Headly, and Sheline [24], Spear [25], and that of Raman et al. [14] are excellent illustrations of how truly important such work can be.

Fourthly, the almost incredible success of VCSs for so many observables over such broad ranges of nuclei and wide variations in structure, presents a real challenge to microscopic nuclear theories to devise a simple and sufficiently general explanation of such simple and general behavior. If this and related challenges can be met, it argues well for a significant improvement and deepening in our understanding of nuclear structure and its evolution.

Acknowledgements

Numerous discussions and collaborations with D. S. Brenner, W.-T. Chou, P. von Brentano, J.-Y. Zhang, K. Heyde, and P. Haustein are gratefully acknowledged. Research has been performed under contracts No. DE-AC02-76CH00016 and DE-FG02-88ER40417 with the United States Department of Energy.

References

[1] Casten R F 1985 *Nucl. Phys.* **A443** 1
[2] Casten R F 1981 *Phys. Rev. Lett.* **47** 1433
[3] Casten R F *et al.* 1987 *Phys. Rev. Lett.* **58** 658
[4] Brenner D S *et al.* 1992 *Phys. Lett.* (in press)
[5] Haustein P E *et al.* 1988 *Phys. Rev.* **C38** 467
[6] Byrski T *et al.* 1990 *Phys. Rev. Lett.* **64** 1650
[7] Stephens F S *et al.* 1990 *Phys. Rev. Lett.* **64** 2623
[8] Ahmad I *et al.* 1991 *Phys. Rev.* **C44** 1206
[9] Baktash C *et al.* 1992 *Phys. Rev. Lett.* **69** 1500
[10] Zhang J Y and Riedinger L L 1992 (preprint)
[11] Casten R F *et al.* 1992 *Phys. Rev.* **C45** R1413
[12] Zhang J Y *et al.* 1992 *Phys. Rev. Lett.* **69** 1160
[13] Mowbray A S *et al.* 1990 *Phys. Rev.* **C42** 1126
[14] Raman S *et al.* 1987 *At. Data and Nucl. Data Tables* **36** 1
[15] Hendrie D L *et al.* 1968 *Phys. Lett.* **26B** 27; Bemis C E *et al.* 1973 *Phys. Rev.* **C8** 1466

[16] Ronningen R M *et al.* 1981 *Phys. Rev. Lett.* **47** 635; Erb K *et al.* 1972 *Phys. Rev. Lett.* **29** 1010
[17] Lister C J *et al.* 1992 *Phys. Rev. Lett.* **49** 308
[18] Raman S *et al.* 1988 *Phys. Rev.* **C37** 805
[19] Frank W *et al.* 1990 *J. Phys.* **G16** L7
[20] Zamfir N V *et al.* 1989 *Phys. Lett.* **B226** 11
[21] Zamfir N V *et al.* 1992 *Annalen Phys.* **2** 71
[22] Casten R F *et al.* 1991 *Los Alamos Report* LALP 91-51
[23] Sakai M 1984 *At. Data and Nucl. Data Tables* **31** 399
[24] Sood P C *et al.* 1991 *At. Data and Nucl. Data Tables* **47** 89
[25] Spear R H 1989 *At. Data and Nucl. Data Tables* **42** 55

DISCLAIMER